https://doi.org/10.5194/egusphere-2026-4276
Preprint. Discussion started: 20 August 2026

Monsoon-driven variability in carbonaceous aerosol sources, chemistry, and optical properties over the equatorial Indian Ocean

Krishnakant Babanrao Budhavant[1*], Ahmed Muslim[2], Joakim Romson[3], Sreedharan Krishnakumari Satheesh[1], Örjan Gustafsson[3*]

[1]Divecha Centre for Climate Change, Indian Institute of Science, Bangalore 560012, India
[2]Maldives Meteorological Service, Gan, Addu City, 19070, Maldives
[3]Department of Environmental Science and the Bolin Centre for Climate Research, Stockholm University, Stockholm 10691, Sweden

Correspondence to: Krishnakant B. Budhavant, Örjan Gustafsson (kbbudhavant@gmail.com, orjan.gustafsson@aces.su.se)

Abstract. Carbonaceous aerosols over the equatorial Indian Ocean influence regional radiative forcing and long-range transport, yet integrated observations linking aerosol chemistry, optical properties, transport pathways, and source characteristics remain scarce. Here, we present year-round measurements of $PM_{2.5}$ chemical composition, aerosol optical properties, air-mass transport, and representative dual-carbon isotope signatures from the Maldives Climate Observatory at Gan (MCOG; 0.69° S, 73.15° E) to investigate how seasonal monsoon circulation regulates aerosol transport and atmospheric processing.

During the northeast monsoon (NEM), continental outflow from South and Southeast Asia resulted in significantly higher $PM_{2.5}$ concentrations (5.6 ± 2.7 μg m^{-3}), aerosol optical depth ($AOD_{500} = 0.17 \pm 0.09$), and elevated concentrations of black carbon (BC), organic carbon (OC), and non-sea-salt sulfate (nss-SO_4^{2-}). In contrast, marine inflow during the southwest monsoon (SWM), together with enhanced precipitation, substantially reduced aerosol loading while increasing the relative contribution of sea-salt aerosol. Diagnostic aerosol ratios revealed significant seasonal shifts in aerosol source characteristics and chemical composition. Although BC mass absorption cross-sections at 658 nm were slightly higher during the SWM, the seasonal difference was not statistically significant. Representative dual-carbon isotope measurements provided independent evidence for mixed fossil and contemporary carbon sources.

These observations demonstrate that monsoon circulation governs aerosol transport, loading, and chemical composition over the equatorial Indian Ocean and provide observational benchmarks for improving the representation of long-range aerosol transport, atmospheric processing, and aerosol–climate interactions in regional chemical transport and Earth system models.

Keywords: Aerosol optical depth; Black carbon; Chemical composition; Source apportionment; Long-range transport; Monsoon transport; South Asia.

https://doi.org/10.5194/egusphere-2026-4276
Preprint. Discussion started: 20 August 2026

Graphical Abstract:

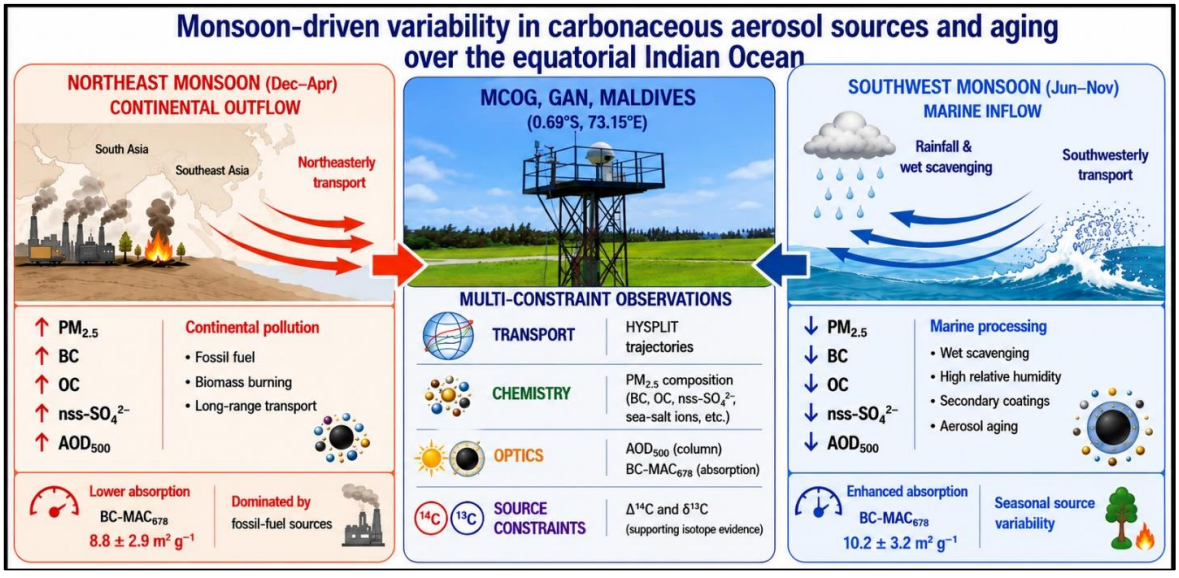

Schematic overview of the monsoon-driven evolution of carbonaceous aerosols over the equatorial Indian Ocean. Continental outflow during the northeast monsoon enhances aerosol loading and the abundance of combustion-derived carbonaceous aerosols. In contrast, marine inflow during the southwest monsoon promotes wet scavenging, atmospheric aging, and enhanced black carbon absorption. The integrated observations of transport, aerosol chemistry, optical properties, and supporting dual-carbon isotope measurements demonstrate how monsoon circulation regulates aerosol sources, atmospheric processing, and aerosol–climate interactions.

1. Introduction

Carbonaceous aerosols are among the most important atmospheric constituents influencing air quality, climate, and the global carbon cycle. Black carbon (BC) strongly absorbs solar radiation and contributes to atmospheric warming, whereas organic carbon (OC) exerts more complex radiative effects through both scattering and absorption depending on its composition and atmospheric evolution. Beyond their direct radiative impacts, carbonaceous aerosols modify cloud microphysics, influence precipitation processes, affect atmospheric chemistry, and contribute to regional climate variability (Bond et al., 2013; IPCC, 2021).

The climatic effects of aerosols are particularly important over the Indian Ocean, where long-range transport of continental aerosols interacts with the seasonally reversing South Asian monsoon circulation. During the northeast monsoon (NEM), persistent northeasterly winds transport anthropogenic emissions, biomass-burning aerosols, and secondary pollutants from South and Southeast Asia across the Indian Ocean. In contrast, the southwest monsoon (SWM) introduces relatively clean marine air masses from the southern Indian Ocean, accompanied by increased precipitation, high relative humidity, and efficient wet scavenging. This seasonal reversal produces pronounced variations in aerosol loading, composition, and atmospheric processing, making the

https://doi.org/10.5194/egusphere-2026-4276
Preprint. Discussion started: 20 August 2026

region a natural laboratory for investigating the evolution of carbonaceous aerosols during long-range transport (Ramanathan et al., 2001; Corrigan et al., 2006; Bosch et al., 2014; Budhavant et al., 2015, 2020).

Although numerous studies have characterized aerosol composition and transport over the northern Indian Ocean, significant uncertainties remain regarding the processes controlling the seasonal evolution of carbonaceous aerosols over the equatorial Indian Ocean (Novakov et al., 2000; Sheesley et al., 2012; Budhavant et al., 2015, 2018). Most previous investigations have focused on aerosol mass concentrations, chemical composition, or source apportionment in isolation, whereas relatively few studies have simultaneously examined transport pathways, aerosol chemistry, optical properties, and carbon-isotope signatures within a single observational framework (Budhavant et al., 2020, 2023). Consequently, the processes linking monsoon-driven transport, atmospheric aging, aerosol optical properties, and carbon source variability remain insufficiently understood.

Atmospheric processing plays a critical role in determining the climatic impacts of carbonaceous aerosols. During long-range transport, BC particles undergo physical and chemical transformations through condensation of secondary inorganic and organic species, heterogeneous reactions, cloud processing, and interactions with water vapor. These processes modify particle mixing state and morphology, enhancing light absorption and altering aerosol radiative forcing (Bond et al., 2013; Liu et al., 2017). Wet scavenging substantially reduces aerosol loading while simultaneously altering aerosol composition. However, continued atmospheric aging during marine transport enhances particle mixing and BC absorption efficiency (Budhavant et al., 2020, 2023). Consequently, aerosol optical properties cannot be inferred solely from BC mass concentrations but must also account for atmospheric aging, particle mixing state, and transport history. Reliable identification of aerosol sources is equally important for understanding atmospheric evolution. Carbon isotope measurements provide valuable constraints on the relative contributions of fossil and contemporary carbon sources, complementing conventional chemical tracers and transport analyses. However, because radiocarbon analyses are analytically demanding and generally available only for selected samples, isotope observations are most powerful when interpreted alongside year-round measurements of aerosol chemistry, optical properties, and air-mass transport. Such a multi-constraint approach enables a more robust interpretation of seasonal source variability than any single observational technique alone.

The Maldives Climate Observatory at Gan (MCOG) occupies a unique receptor location in the equatorial Indian Ocean, where seasonally reversing monsoon circulation alternately transports polluted continental outflow from South and Southeast Asia during the NEM and predominantly marine air masses from the southern Indian Ocean during the SWM (Figure 1). This pronounced seasonal contrast provides an ideal natural laboratory for investigating how monsoon circulation regulates aerosol transport, chemical composition, atmospheric aging, and optical properties during long-range transport. As one of the few long-term atmospheric observatories in the equatorial Indian Ocean, MCOG offers a unique observational platform for quantifying the seasonal evolution of carbonaceous aerosols and their implications for regional aerosol–climate interactions.

In this study, we present year-round observations of $PM_{2.5}$ chemical composition, aerosol optical properties, air-mass transport, and representative dual-carbon-isotope measurements collected at MCOG in 2022. By integrating these complementary datasets, we investigate the mechanisms through which seasonal monsoon circulation influences aerosol transport, source characteristics, atmospheric aging, and BC absorption over the equatorial Indian Ocean.

https://doi.org/10.5194/egusphere-2026-4276
Preprint. Discussion started: 20 August 2026

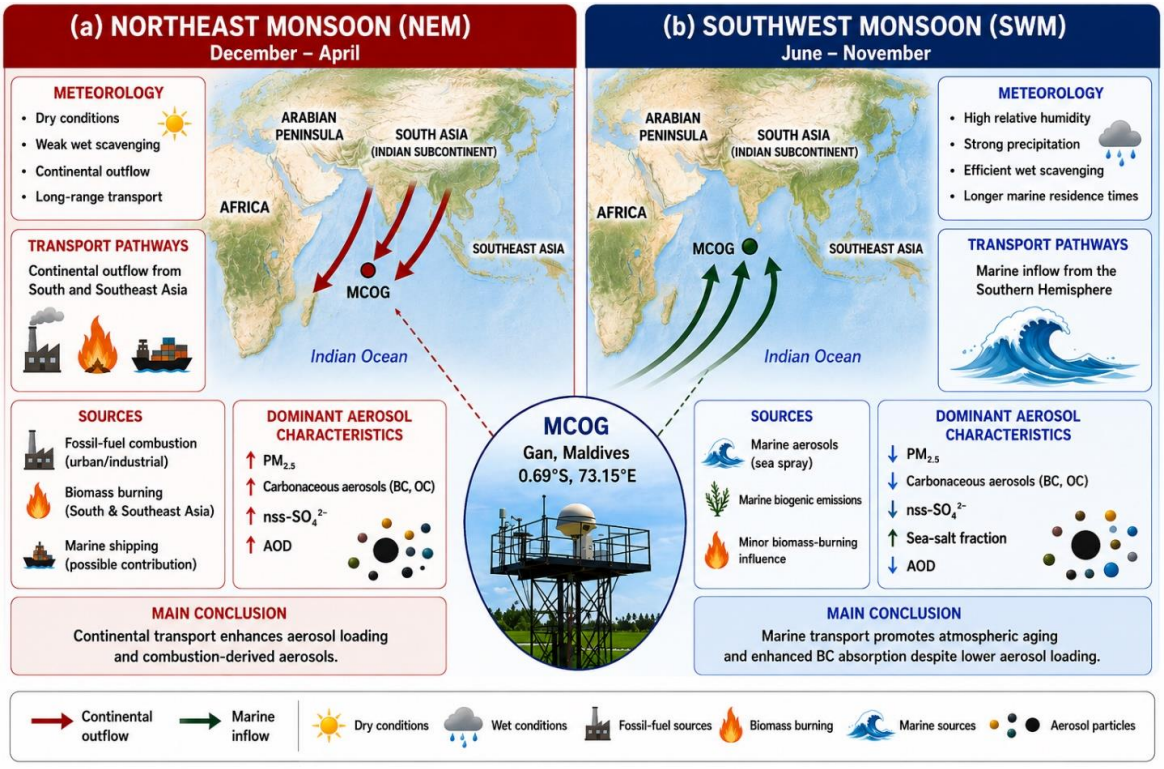

Figure 1: Conceptual framework illustrating the contrasting aerosol regimes associated with the northeast monsoon (NEM) and southwest monsoon (SWM) over the equatorial Indian Ocean. During the NEM, continental outflow from South and Southeast Asia transports combustion-derived aerosols, resulting in enhanced aerosol loading, carbonaceous aerosol concentrations, non-sea-salt sulfate, and aerosol optical depth. During the SWM, marine inflow from the southern Indian Ocean is characterized by higher relative humidity, increased precipitation, efficient wet scavenging, and a greater relative contribution of sea-salt aerosol. The Maldives Climate Observatory at Gan (MCOG) serves as a unique receptor site for investigating monsoon-driven variability in aerosol transport, chemical composition, atmospheric processing, optical properties, and source characteristics over the equatorial Indian Ocean.

Specifically, this study addresses the following hypotheses:

1. Seasonal monsoon circulation governs air-mass transport pathways and aerosol loading over the equatorial Indian Ocean.
2. Changes in transport pathways modify aerosol chemical composition and promote atmospheric aging, thereby enhancing BC absorption during marine transport.
3. Representative dual-carbon isotope measurements provide complementary evidence supporting seasonal variability in carbon source contributions inferred from transport and aerosol chemistry.

By combining transport analysis, aerosol chemistry, optical properties, and supporting isotope observations within a unified observational framework, this study provides new insights into the processes governing the evolution of monsoon-driven aerosols over the equatorial Indian Ocean. The results improve our understanding of aerosol transport and atmospheric aging in this

https://doi.org/10.5194/egusphere-2026-4276
Preprint. Discussion started: 20 August 2026

climatically important region and provide observational constraints for improving the representation of aerosol–climate interactions in regional chemical transport and Earth system models.

2 Methods

2.1 Site description and aerosol sampling

Atmospheric aerosol measurements were conducted at the MCOG (0.69° S, 73.15° E, 5 m above mean sea level), located on Gan Island in Addu Atoll, the southernmost atoll of the Maldives in the equatorial Indian Ocean (Figure 2). $PM_{2.5}$ aerosol samples were collected throughout 2022 using a high-volume aerosol sampler installed on the atmospheric sampling tower at MCOG. Sampling was conducted on a regular schedule to capture the full seasonal cycle, including both the NEM (December to April) and the SWM (June to October), as well as transitional periods. The observatory provides long-term atmospheric measurements to investigate regional aerosol transport and seasonal variability over the equatorial Indian Ocean.

Fine particulate matter ($PM_{2.5}$) was collected using a high-volume aerosol sampler (Digitel DH-77, Digitel Elektronik AG, Switzerland) equipped with a $PM_{2.5}$ size-selective inlet (impactor with silicone-greased plate) and operated at a nominal flow rate of 500 ± 10 L min^{-1}. Aerosol particles were collected on binder-free quartz filters (Millipore AQFA8X105, Merck, Ireland) cut to 150 mm diameter, which were pre-combusted by heating at 450 °C for 6 h before sampling, to remove residual organic contaminants. The filters were kept in pre-combusted, folded aluminum foil envelopes and then sealed in polyethylene bags. Before and after sampling, filters were weighed in a climate-controlled room (20 °C, 50% RH) after at least 24 h of equilibration. Samples were stored at -20 °C except during transport and analysis. Aerosol sampling was performed continuously throughout the year, using 72-hour integrated sampling periods. The extended sampling duration was selected to obtain sufficient particulate mass for comprehensive analyses of carbonaceous components, inorganic ions, optical properties, and dual-carbon-isotope compositions, while maintaining adequate temporal resolution to resolve seasonal and monsoon-scale variability.

Instrument flow rates were calibrated regularly using a certified flow calibration system. Field blank filters were collected at regular intervals, handled identically to exposed samples except for active air sampling, and used to evaluate potential contamination during filter handling, transport, and laboratory processing.

2.2 Carbonaceous aerosols and chemical composition

Carbonaceous aerosol components, including OC and elemental carbon (EC), hereafter referred to as BC, were quantified using a thermal–optical carbon analyzer (Model 4L, Sunset Laboratory Inc., USA) following the NIOSH 5040 protocol. During analysis, filter punches (1.5 cm^2) were subjected to a stepwise temperature program under helium and helium–oxygen atmospheres. Desorbed carbon during the helium phase was oxidized to CO_2 in an MnO_2 oven, and the remaining carbon was directly combusted during the helium-oxygen phase before passing through the MnO_2 oven. CO_2 was quantified with a flame ionization detector (FID) after conversion to CH_4 in a methanator. Continuous laser transmittance (658 nm) measurements were used to correct for pyrolytic carbon formation and to determine the OC–BC split point. Instrument calibration was performed using NIST-traceable (SRM

https://doi.org/10.5194/egusphere-2026-4276
Preprint. Discussion started: 20 August 2026

8785) sucrose standards, and routine quality control included calibration verification, replicate analyses, and blank corrections. Based on repeated analyses and calibration performance, the analytical uncertainties were estimated to be approximately ±10% for OC and ±15% for BC. Further details are provided in Budhavant et al. (2015, 2023).

Major water-soluble inorganic ions, Na^+, K^+, Ca^{2+}, Mg^{2+}, NH_4^+, Cl^-, NO_3^-, and SO_4^{2-}, were measured by ion chromatography (Dionex Aquion system, Thermo Fisher Scientific, USA). Filter punches were extracted in Milli-Q water (18.2 MΩ·cm, 0.22 µm filter) in 15-mL polypropylene centrifuge tubes and sonicated for 30 min prior to analysis. Anions were separated on an AS9-HC column, and cations on a CS12A column. Analytical precision for ion concentrations was typically better than 5%; detection limits were <0.1 µg m^{-3}. More details are provided in Budhavant et al. (2023). To distinguish marine and non-marine contributions, concentrations of non-sea-salt sulfate (nss-SO_4^{2-}), non-sea-salt potassium (nss-K^+), non-sea-salt calcium (nss-Ca^{2+}), and non-sea-salt magnesium (nss-Mg^{2+}) were calculated using sodium (Na^+) as a conservative tracer of sea salt and the corresponding seawater ionic ratios following Keene et al. (1986).

$$\text{nss-X} = X_{measured} - Na^+ \times (X/Na^+)_{seawater}$$

where X denotes SO_4^{2-}, K^+, Ca^{2+} and Mg^{2+}. Organic matter (OM) concentrations were estimated from measured OC using an OM/OC conversion factor of 1.8, consistent with previous observations of aged continental aerosols transported over the Indian Ocean and South Asian outflow regions (Turpin and Lim, 2001; Budhavant et al., 2015, 2018). The selected conversion factor falls within the range commonly reported for moderately to highly oxidized atmospheric organic aerosols. It provides a reasonable estimate of particulate organic matter for regional mass closure.

Analytical uncertainties associated with carbonaceous species, inorganic ions, and derived parameters were propagated throughout subsequent calculations. The combined uncertainties associated with OM estimation and non-sea-salt calculations were substantially smaller than the observed seasonal differences and therefore do not influence the principal interpretation of monsoon-driven changes in aerosol composition and source characteristics.

2.3 Aerosol optical properties

The optical properties of carbonaceous aerosols were characterized using the BC mass absorption cross-section (BC-MAC_{658}) and column-integrated aerosol optical depth (AOD). These complementary measurements provide information on aerosol absorption efficiency at the surface and the total atmospheric aerosol loading, respectively.

The BC-MAC_{658} was estimated from filter-based optical attenuation measurements obtained using the Sunset Laboratory thermal–optical carbon analyzer. Optical attenuation at the instrument laser wavelength (658 nm) was measured continuously during thermal analysis and combined with thermally determined BC mass concentrations to estimate BC-MAC_{658} following approaches previously applied over the Indian Ocean (Ram and Sarin, 2009; Budhavant et al., 2020, 2024; Nair et al., 2024). The aerosol absorption coefficient was derived from the measured optical attenuation using a multiple-scattering correction factor of 4.5 (Weingartner et al., 2003; Budhavant et al., 2024). BC-MAC_{658} was calculated as the ratio of the aerosol absorption coefficient to the corresponding BC mass concentration. Variations in BC-MAC_{658} were interpreted as indicators of changes in particle mixing

https://doi.org/10.5194/egusphere-2026-4276
Preprint. Discussion started: 20 August 2026

state, secondary aerosol coatings, and atmospheric aging. It should be noted that BC-MAC$_{658}$ provides an indirect measure of atmospheric processing and does not constitute a direct measurement of particle morphology or internal mixing state.

Column-integrated AOD was obtained from a CIMEL sun–sky radiometer operated as part of the Aerosol Robotic Network (AERONET) at MCOH. Only Version 3 Level 2.0 quality-assured data, representing 230 measurement days, were used in this study. The AERONET processing algorithm includes automatic cloud screening, instrument calibration, and standardized quality-control procedures, ensuring high-quality and globally consistent aerosol optical measurements (Holben et al., 1998; Giles et al., 2019). Daily mean AOD at 500 nm (AOD$_{500}$) was used to characterize seasonal changes in column aerosol loading and to complement the surface-based PM$_{2.5}$ observations.

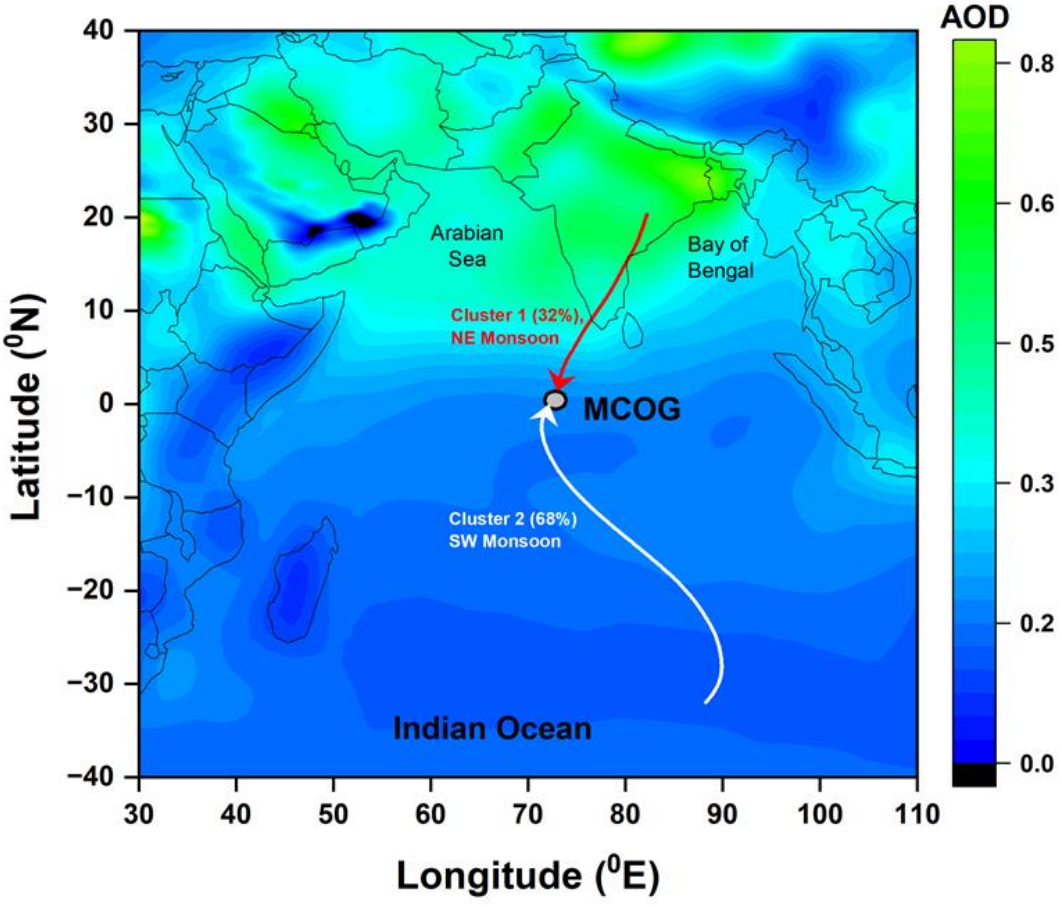

Figure 2: Dominant seasonal transport pathways to the Maldives Climate Observatory at Gan (MCOG), inferred from 10-day HYSPLIT backward-trajectory clusters overlaid on the 2022 MODIS annual aerosol optical depth (AOD) distribution. Continental outflow during the northeast monsoon (red) originates from South and Southeast Asia, whereas air masses dominate marine inflow during the southwest monsoon (blue) from the southern Indian Ocean. Additional details regarding the trajectory clustering are provided in the Supplemental Information (Figure S3).

https://doi.org/10.5194/egusphere-2026-4276
Preprint. Discussion started: 20 August 2026

2.4 Meteorological measurements and air-mass trajectory analysis

Meteorological parameters, including air temperature, relative humidity (RH), precipitation, wind speed, and wind direction, were obtained from the Maldives Meteorological Service station located adjacent to the MCOG. These observations were used to characterize seasonal meteorological conditions and to interpret variations in aerosol loading, chemical composition, optical properties, and atmospheric processing associated with the monsoon circulation.

Air-mass transport pathways were investigated using the Hybrid Single-Particle Lagrangian Integrated Trajectory (HYSPLIT, version 5.4.2) model developed by the NOAA Air Resources Laboratory (Draxler and Hess, 1998; Stein et al., 2015). Ten-day backward trajectories were calculated four times daily (00:00, 06:00, 12:00, and 18:00 UTC) using an arrival height of 50 m above ground level, consistent with previous trajectory analyses at the MCOG that focused on near-surface marine air masses (e.g., Budhavant et al., 2024). Meteorological input fields were obtained from the Global Data Assimilation System (GDAS) with a horizontal resolution of 1° × 1°. The 10-day trajectory length was selected to capture long-range transport from major continental and marine source regions.

Trajectory clustering was performed using the Total Spatial Variance (TSV) method implemented within HYSPLIT to identify the dominant transport regimes and reduce trajectory complexity. Two major trajectory clusters were identified, representing continental and marine transport pathways (Figure S3), and were subsequently used to interpret seasonal variations in aerosol chemistry, optical properties, and isotope signatures. Although uncertainties in individual trajectories increase with transport time, the ensemble trajectory analysis provides a robust characterization of the dominant seasonal transport patterns influencing MCOG.

2.5 Dual-carbon isotope measurements and analysis

A subset of $PM_{2.5}$ samples was selected for dual-carbon isotope analysis. The selected samples were collected during each monsoon season and had relatively high BC concentrations to ensure sufficient carbon mass for accurate radiocarbon ($\Delta^{14}C$) and stable carbon isotope ($\delta^{13}C$) measurements. BC was isolated from quartz fiber filters using the thermal–optical transmission method described previously, coupled with online CO_2 collection following established procedures (Zencak et al., 2007; Chen et al., 2013; Andersson et al., 2015; Budhavant et al., 2015, 2023). During thermal–optical analysis, the BC fraction was evolved under controlled heating conditions, and the resulting CO_2 was purified using magnesium perchlorate and silver wool traps to remove water vapor and halogen-containing gases, respectively. The purified CO_2 was cryogenically trapped in liquid nitrogen and flame-sealed in pre-combusted borosilicate glass ampoules for isotope analysis.

Radiocarbon ($\Delta^{14}C$) and stable carbon isotope ($\delta^{13}C$) measurements were performed at the Department of Physics and Astronomy, Uppsala University, Sweden. Radiocarbon signatures were used to distinguish fossil-fuel-derived BC ($\Delta^{14}C \approx -1000‰$) from contemporary biomass-derived carbon, while $\delta^{13}C$ provided complementary information on carbon source characteristics and atmospheric processing (Gustafsson et al., 2009; Bosch et al., 2014; Kirillova et al., 2013, 2014; Andersson et al., 2015; Budhavant et al., 2023). The combined use of $\Delta^{14}C$ and $\delta^{13}C$ provides a robust source-diagnostic framework for evaluating seasonal variability in BC sources over the equatorial Indian Ocean.

https://doi.org/10.5194/egusphere-2026-4276
Preprint. Discussion started: 20 August 2026

Seasonal differences between the NEM and SWM were evaluated using Welch's t-test and Mann–Whitney U test. Statistical significance was defined as $p < 0.05$.

3. Results and discussion

3.1 Monsoon meteorology, transport pathways, and aerosol loading

Seasonal meteorological conditions over the equatorial Indian Ocean during 2022 exhibited the characteristic reversal associated with the South Asian monsoon system (Figures S1 and S2). During the NEM, relatively dry conditions and persistent northeasterly winds favoured the transport of continental air masses from South and Southeast Asia. In contrast, the SWM was characterized by stronger southwesterly winds, higher relative humidity, and substantially greater precipitation, reflecting the increased influence of marine air masses originating over the southern Indian Ocean.

The contrasting meteorological regimes were clearly reflected in the HYSPLIT backward trajectories (Figure 2). During the NEM, air masses predominantly originated over South and Southeast Asia before reaching MCOG, whereas during the SWM trajectories remained largely confined to the southern Indian Ocean, indicating a predominantly marine influence. Trajectory cluster analysis further showed that continental transport accounted for approximately 32 % of all air masses arriving at MCOG, while marine transport represented the remaining 68 % (Figure S3). Continental trajectories crossed densely populated and industrialized regions where anthropogenic emissions, biomass burning, and secondary aerosol formation are major aerosol sources, whereas marine trajectories originated over the remote southern Indian Ocean and were associated with comparatively clean oceanic air masses.

The MODIS annual AOD distribution independently supports these transport patterns (Figure 2). Elevated aerosol loading over the Indo-Gangetic Plain, northern Indian Ocean, and parts of Southeast Asia coincided with the principal continental transport pathways during the NEM, whereas substantially lower AOD over the southern Indian Ocean was consistent with the predominantly marine trajectories observed during the SWM. The close agreement between satellite observations and HYSPLIT trajectories indicates that the seasonal monsoon circulation strongly influences the transport pathways by which aerosols reach the equatorial Indian Ocean.

These contrasting transport regimes were reflected in the observed aerosol loading. $PM_{2.5}$ concentrations exhibited a pronounced seasonal cycle, averaging 5.6 ± 2.7 μg m^{-3} during the NEM and decreasing significantly to 3.3 ± 1.3 μg m^{-3} during the SWM ($p < 0.001$; Table 1, Figure 3). A similar seasonal pattern was observed for AOD_{500}, which decreased significantly from 0.17 ± 0.09 during the NEM to 0.11 ± 0.04 during the SWM ($p < 0.001$; Table 1, Figure 4). The consistent seasonal behaviour of surface $PM_{2.5}$, column-integrated AOD, backward trajectories, and satellite observations demonstrates that monsoon-driven changes in regional transport largely determine aerosol loading over the equatorial Indian Ocean. During the SWM, aerosol concentrations were significantly lower, yet measurable $PM_{2.5}$ levels persisted throughout the year. This indicates that long-range transport continued to be an important contributor to the regional background aerosol burden in both continental and marine conditions.

Table 1. Summary of aerosol properties measured at the Maldives Climate Observatory-Gan during December 2021 to January 2023. Reported parameters include sampling period, aerosol optical depth (AOD), number of samples, $PM_{2.5}$ mass concentration and mass absorption cross-sections of black carbon at 658 nm ($BC–MAC_{658}$), BC, organic carbon (OC), and major inorganic ions.

Sampling period	AOD	No. of samples	$PM_{2.5}$ ($\mu g\ m^{-3}$)	$BC\text{-}MAC_{658}$ ($m^2\ g^{-1}$)	BC ($\mu g\ m^{-3}$)	OC ($\mu g\ m^{-3}$)	$nss\text{-}SO_4^{2-}$ ($\mu g\ m^{-3}$)	NO_3^- ($ng\ m^{-3}$)	$nss\text{-}K^+$ ($ng\ m^{-3}$)	$nss\text{-}Ca^{2+}$ ($ng\ m^{-3}$)	$nss\text{-}Br^-$ ($ng\ m^{-3}$)
NE monsoon	0.17 ± 0.09	46	5.59 ± 2.7	8.81 ± 2.87	0.21 ± 0.18	0.65 ± 0.70	1.32 ± 0.7	24 ± 9	90 ± 63	47 ± 43	28 ± 17
Pre-transition	0.10 ± 0.04	8	2.79 ± 1.0	9.53 ± 2.31	0.04 ± 0.03	0.18 ± 0.13	0.52 ± 0.3	18 ± 4	25 ± 15	51 ± 46	42 ± 14
SW Monsoon	0.11 ± 0.04	26	3.29 ± 1.3	10.2 ± 3.18	0.05 ± 0.05	0.23 ± 0.19	0.50 ± 0.4	24 ± 10	27 ± 34	27 ± 33	41 ± 25
Post-transition	0.11 ± 0.04	7	2.65 ± 1.4	8.65 ± 2.54	0.05 ± 0.02	0.17 ± 0.03	0.44 ± 0.3	21 ± 4	19 ± 12	13 ± 9	48 ± 17
Annual	0.14 ± 0.08	87	4.41 ± 2.5	9.28 ± 2.90	0.14 ± 0.15	0.44 ± 0.46	0.93 ± 0.7	23 ± 9	60 ± 59	39 ± 39	35 ± 19

https://doi.org/10.5194/egusphere-2026-4276
Preprint. Discussion started: 20 August 2026

3.2 Monsoon-driven changes in aerosol chemistry and source signatures

3.2.1 Seasonal variability in aerosol chemical composition

The pronounced seasonal differences in aerosol loading were accompanied by significant changes in aerosol chemical composition, reflecting the alternating influence of continental outflow and marine inflow associated with the South Asian monsoon (Figure 3; Table 1). Carbonaceous aerosol components and secondary inorganic species were substantially enhanced during the NEM, whereas marine-derived constituents became relatively more important during the SWM. The pre- and post-monsoon transition periods exhibited intermediate chemical characteristics, reflecting the progressive replacement of continental air masses by marine inflow during monsoon onset and the gradual re-establishment of continental influence during monsoon withdrawal.

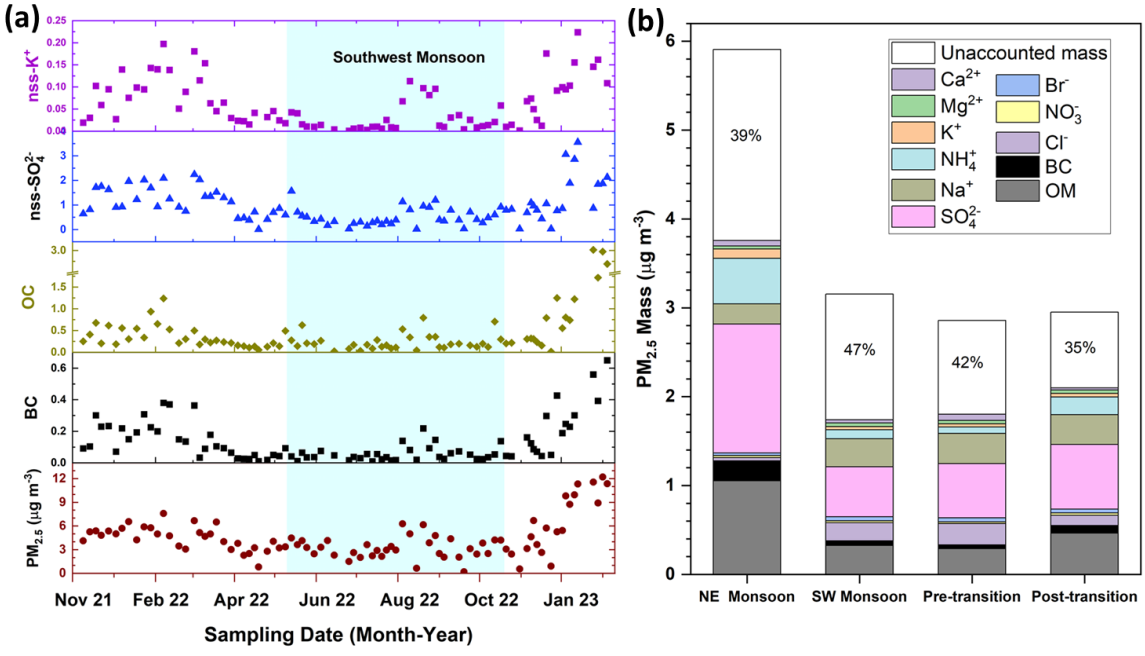

Figure 3: Panel (A) Time series of $PM_{2.5}$ mass concentration and major aerosol chemical components measured at the Maldives Climate Observatory at Gan (MCOG) during 2022, including elemental carbon (BC), organic matter (OM), non-sea-salt sulfate (nss-SO_4^{2-}), and non-sea-salt potassium (nss-K^+). The cyan-shaded region denotes the southwest monsoon (SWM). (B) Mean chemical composition of $PM_{2.5}$ during the northeast monsoon (NEM), pre-transition, SWM, and post-transition periods, showing the relative contributions of water-soluble inorganic ions, carbonaceous components (OM and BC), and the unidentified residual fraction.

Concentrations of BC, OC, OM, and nss-SO_4^{2-} were all significantly higher during the NEM than during the SWM ($p < 0.001$; Table 1). The transition periods generally showed intermediate concentrations, consistent with the gradual evolution of air-mass origin rather than abrupt changes in aerosol composition. Elevated concentrations of carbonaceous aerosols and nss-SO_4^{2-} during the NEM are consistent with efficient long-range transport of combustion-derived aerosols and secondary sulfate from South and Southeast Asia. These observations agree with previous studies over the northern Indian Ocean and South Asian outflow, which

https://doi.org/10.5194/egusphere-2026-4276
Preprint. Discussion started: 20 August 2026

have demonstrated enhanced transport of anthropogenic aerosols during the winter monsoon (Ramanathan et al., 2001; Stone et al., 2007; Budhavant et al., 2020, 2023; Clarke et al., 2026).

Although the absolute concentrations of sea-salt ions also varied seasonally, the relative contributions of Na^+ and Cl^- to $PM_{2.5}$ increased significantly during the SWM ($p < 0.05$), indicating a transition from a pollution-dominated aerosol regime during the NEM to a more marine-influenced aerosol composition. The transition periods bridged these contrasting seasonal regimes, with continental tracers progressively decreasing at monsoon onset and increasing at monsoon withdrawal, reflecting the seasonal evolution of transport pathways.

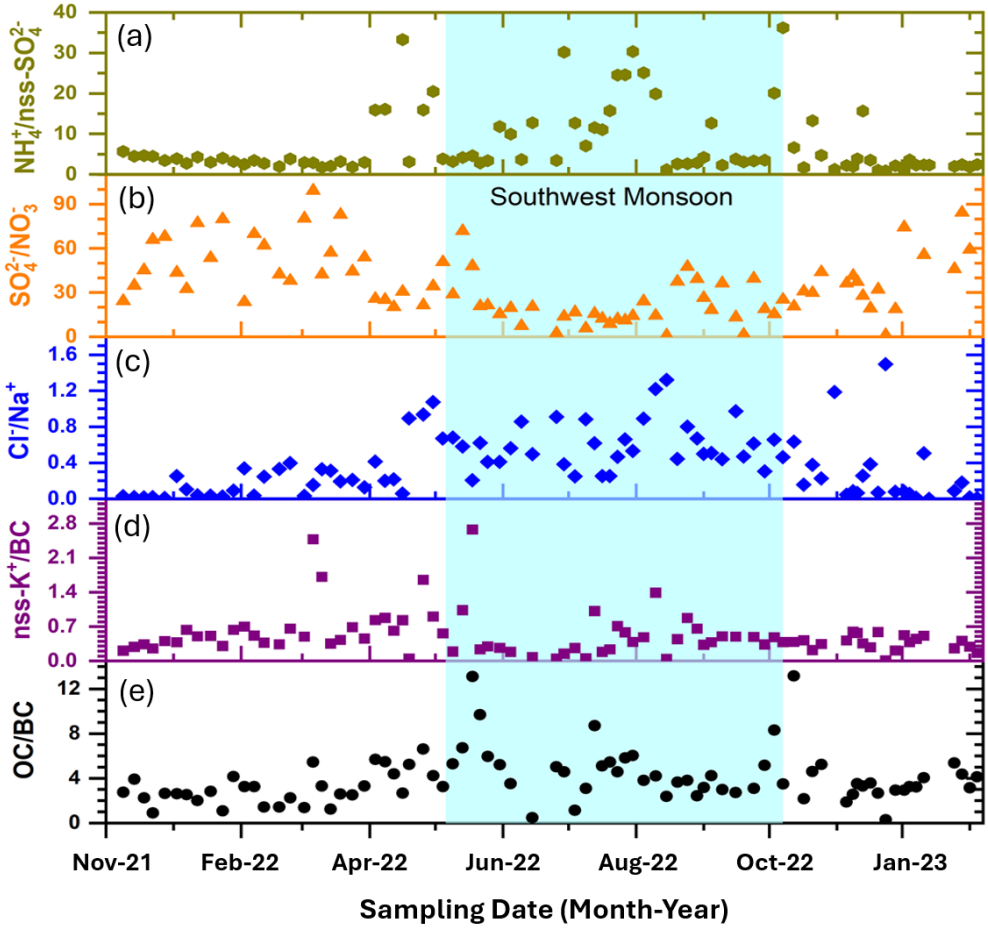

Figure 4: Seasonal variability of aerosol diagnostic ratios measured at the Maldives Climate Observatory at Gan (MCOG) during December 2021–January 2023: (a) NH_4^+/nss-SO_4^{2-}, (b) nss-SO_4^{2-}/NO_3^-, (c) Cl^-/Na^+, (d) nss-K^+/BC, and (e) OC/BC. Shaded regions denote the northeast monsoon (NEM), southwest monsoon (SWM), and the intervening transition periods. The seasonal evolution of these diagnostic ratios illustrates changes in the relative influence of continental and marine aerosol sources, secondary aerosol composition, and aerosol source characteristics associated with monsoon-driven transport over the equatorial Indian Ocean.

https://doi.org/10.5194/egusphere-2026-4276
Preprint. Discussion started: 20 August 2026

3.2.2 Diagnostic aerosol ratios and evidence for source variability

Diagnostic aerosol ratios provide additional insight into seasonal variations in aerosol sources and chemical processing beyond what concentration measurements alone can provide (Figure 4). Seasonal correlation patterns among major aerosol species further support these changes in aerosol composition and source characteristics (Figure S4).

The OC/BC ratio was significantly higher during the SWM than during the NEM (3.22 ± 1.97 vs. 4.89 ± 2.67; Mann–Whitney $p < 0.001$; Figure 4e), indicating a greater relative contribution of organic carbon under marine conditions. Conversely, lower OC/BC ratios during the NEM are consistent with stronger influences of combustion-derived continental aerosols transported from South and Southeast Asia (Bosch et al., 2014; Budhavant et al., 2015, 2020). The transition periods exhibited intermediate values, reflecting the gradual shift between continental and marine air masses.

The NH_4^+/nss-SO_4^{2-} ratio also differed significantly between the two monsoon seasons ($p < 0.001$; Figure 4a), with higher and more variable values during the SWM. In contrast, the nss-SO_4^{2-}/NO_3^- ratio was significantly higher during the NEM ($p < 0.001$; Figure 4b), confirming the dominance of sulfate over nitrate, particularly during continental outflow. The Cl^-/Na^+ ratio increased significantly during the SWM ($p < 0.001$; Figure 4c), consistent with a stronger contribution of fresh marine sea salt.

The nss-K^+/BC ratio showed considerable temporal variability but no significant seasonal difference (Figure 4d). Consequently, although individual samples suggest episodic biomass-burning influence, this ratio is interpreted only as a qualitative indicator of source variability because non-sea-salt potassium also has non-combustion sources (Safai et al., 2010).

Overall, the diagnostic ratios demonstrate statistically significant seasonal changes in the relative contributions of continental and marine aerosol components, while the transition periods exhibited intermediate characteristics consistent with the gradual evolution of monsoon circulation. Together with the transport analysis and aerosol composition presented in Sections 3.1 and 3.2.1, these results show that seasonal monsoon circulation strongly influences aerosol source characteristics over the equatorial Indian Ocean.

3.3 Atmospheric aging enhances BC absorption over the equatorial Indian Ocean

3.3.1 Seasonal variability in BC-MAC and aerosol optical depth

Aerosol optical properties exhibited contrasting responses to seasonal monsoon circulation (Figure 5; Table 1). The AOD_{500} closely followed the seasonal variation in $PM_{2.5}$, decreasing significantly from 0.17 ± 0.09 during the NEM to 0.11 ± 0.04 during the SWM ($p < 0.001$). This behaviour is consistent with the strong reduction in aerosol loading associated with the transition from continental outflow to predominantly marine air masses.

https://doi.org/10.5194/egusphere-2026-4276
Preprint. Discussion started: 20 August 2026

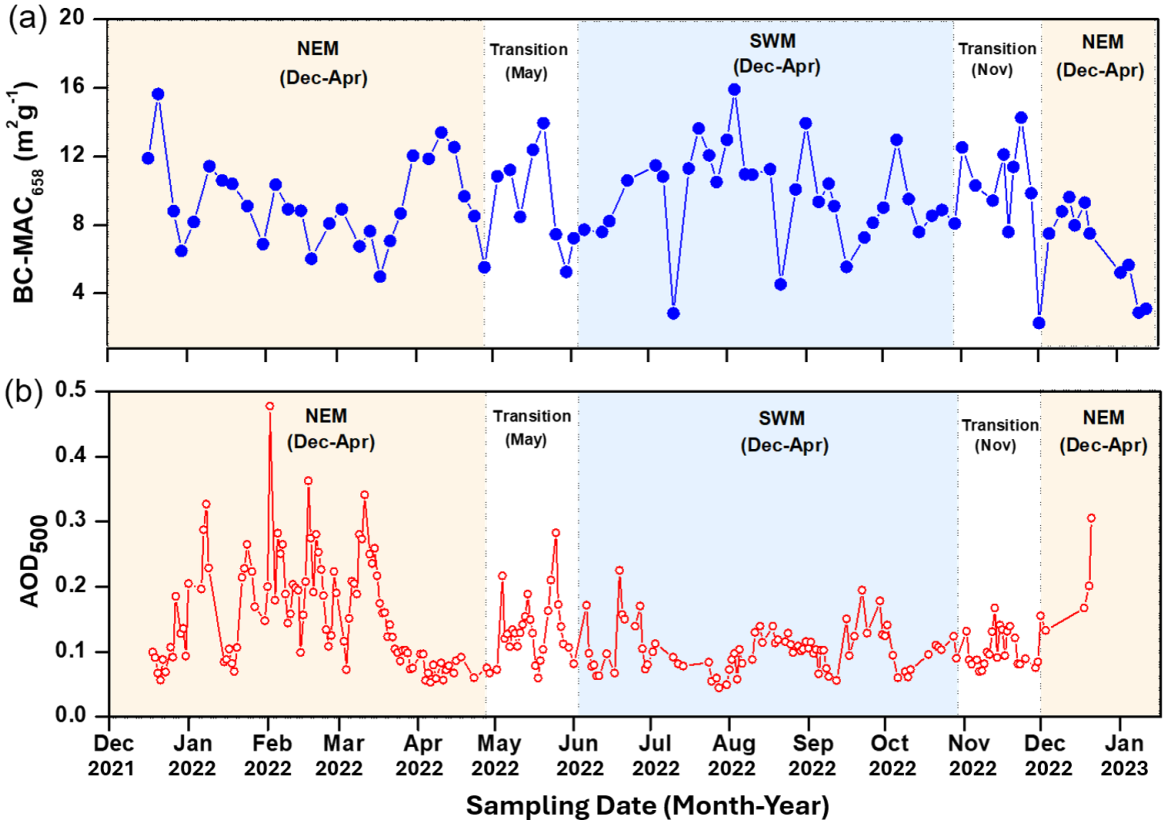

Figure 5: Seasonal variability of (a) black carbon mass absorption cross-section at 658 nm (BC-MAC$_{658}$) and (b) aerosol optical depth at 500 nm (AOD$_{500}$) measured at the Maldives Climate Observatory at Gan (MCOG) from December 2021 to January 2023. Shaded regions denote the northeast monsoon (NEM), southwest monsoon (SWM), and the intervening transition periods. AOD$_{500}$ exhibits a pronounced seasonal cycle, with higher values during the NEM, which correspond to enhanced continental aerosol loading. In contrast, BC-MAC$_{658}$ shows only modest seasonal variability despite the substantial changes in aerosol loading between the two monsoon regimes.

In contrast, BC-MAC$_{658}$ exhibited only modest seasonal variability. Mean BC-MAC$_{658}$ increased from 8.8 ± 2.9 m² g^{-1} during the NEM to 10.2 ± 3.2 m² g^{-1} during the SWM; however, this difference was not statistically significant (Table S1). The substantial overlap between the seasonal distributions indicates that the average light-absorbing efficiency of BC remained broadly comparable under the contrasting monsoon regimes.

The contrasting behaviour of AOD$_{500}$ and BC-MAC$_{658}$ indicates that seasonal monsoon circulation exerted a much stronger influence on aerosol abundance than on the intrinsic absorption efficiency of BC particles. Although the tendency toward higher BC-MAC$_{658}$ during the SWM is consistent with atmospheric processing during marine transport, the absence of a statistically significant seasonal difference suggests that BC absorption efficiency remained relatively stable despite pronounced changes in

https://doi.org/10.5194/egusphere-2026-4276
Preprint. Discussion started: 20 August 2026

aerosol loading. The implications of these observations for atmospheric aging and aerosol radiative effects are discussed in the following section.

3.3.2 Atmospheric processing and implications for BC optical properties

The seasonal evolution of BC optical properties is interpreted in the context of the contrasting meteorological conditions, transport pathways, and aerosol chemistry over the equatorial Indian Ocean. During the SWM, persistently high relative humidity, frequent precipitation, and predominantly marine air masses provide favourable conditions for aqueous-phase oxidation and secondary aerosol formation during long-range transport (Bond et al., 2013; Liu et al., 2017). Although wet deposition efficiently removes a substantial fraction of atmospheric aerosol, the particles that remain airborne continue to undergo chemical processing under humid marine conditions.

The aerosol chemical observations are broadly consistent with this interpretation. Sulfate remained the dominant secondary inorganic aerosol throughout the year, while the significantly higher OC/BC ratios observed during the SWM indicate a greater relative contribution of organic aerosol under marine conditions. In addition, the significantly higher Cl^-/Na^+ ratio during the SWM ($p < 0.001$) reflects the increased influence of relatively fresh marine sea salt. Together, these observations suggest continued atmospheric processing during marine transport, although they do not provide direct evidence of changes in BC particle mixing state or coating thickness.

The HYSPLIT trajectory analysis further shows that SWM air masses traveled predominantly over the southern Indian Ocean before reaching MCOG, providing longer residence times under marine conditions than during the NEM. Such transport pathways favour atmospheric oxidation and particle transformation. However, the seasonal increase in BC-MAC_{658} was modest and not statistically significant (Welch's t-test, $p = 0.103$; Mann–Whitney U test, $p = 0.064$). Consequently, although the observations are consistent with atmospheric processing during transport, they do not conclusively demonstrate enhanced BC absorption associated with aging.

The observed BC-MAC_{658} values nevertheless fall within the range previously reported for aged aerosols over the northern Indian Ocean and South Asian outflow regions (Budhavant et al., 2020, 2024), suggesting that the optical properties of BC at MCOG are representative of the regional background aerosol. The combination of transport analysis, aerosol chemistry, and optical observations indicates that monsoon circulation strongly influences aerosol loading and composition, whereas the average light-absorbing efficiency of BC remains comparatively stable despite pronounced seasonal changes in aerosol abundance.

These findings have important implications for aerosol–climate interactions over the equatorial Indian Ocean. The present observations suggest that accurately representing monsoon-driven transport, wet removal, and seasonal changes in aerosol composition is likely to have a greater influence on model performance than introducing increasingly complex parameterizations of BC absorption efficiency. Nevertheless, longer-term observations combining BC optical measurements with direct characterization of particle mixing state and morphology are needed to determine whether transport-dependent changes in BC optical properties require more sophisticated treatment in regional and global atmospheric models.

https://doi.org/10.5194/egusphere-2026-4276
Preprint. Discussion started: 20 August 2026

3.4. Supporting dual-carbon isotope evidence for aerosol source variability

Dual-carbon isotope measurements were performed on a limited number of $PM_{2.5}$ samples to provide an independent assessment of carbon source characteristics over the equatorial Indian Ocean (Figure 6). Owing to the analytical complexity and high carbon mass requirements of radiocarbon analysis, isotope measurements were restricted to samples with sufficiently high carbon loading. Consequently, the isotope dataset represents a targeted subset of the year-round observations and is interpreted as complementary evidence rather than a comprehensive seasonal source-apportionment dataset.

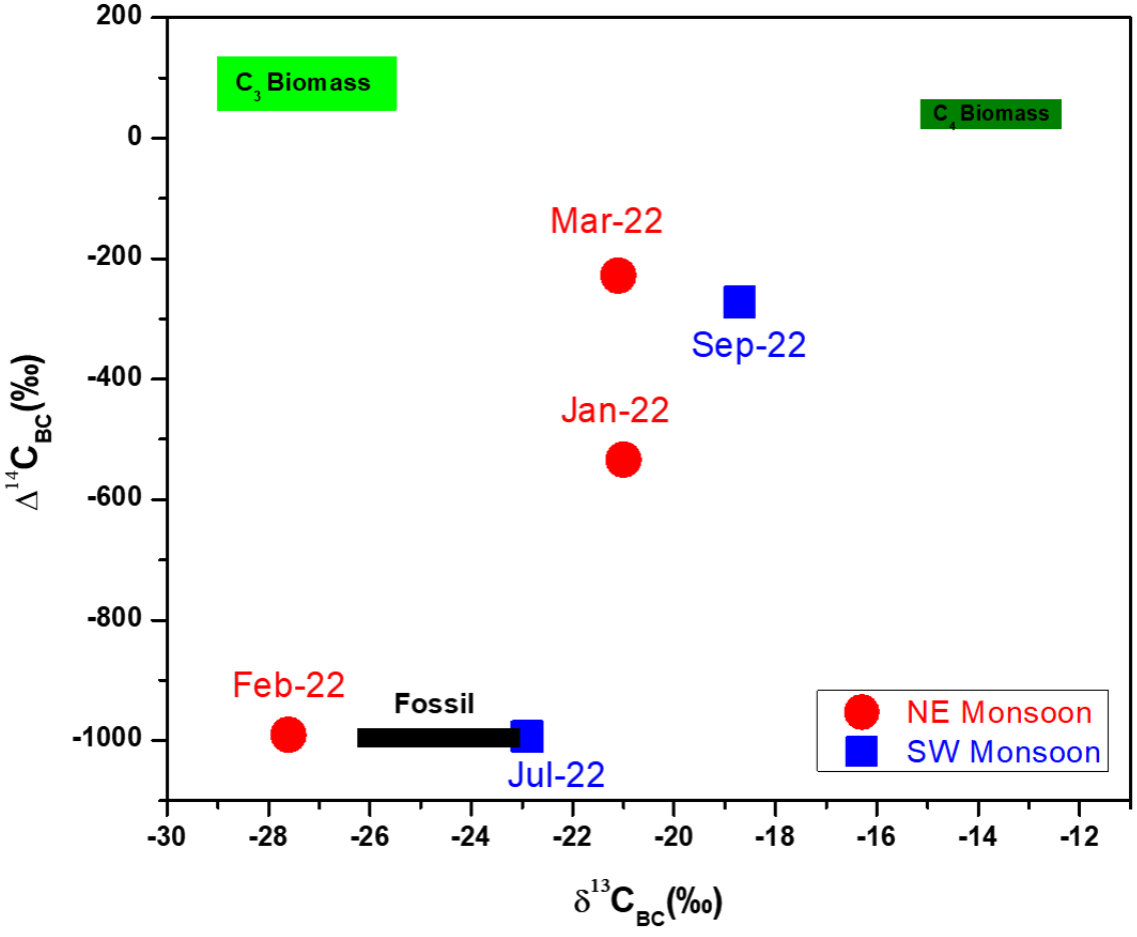

Figure 6: Dual-carbon isotope signatures ($\delta^{13}C$ and $\Delta^{14}C$) of black carbon (BC) measured at the Maldives Climate Observatory at Gan (MCOG). Circles and squares represent samples collected during the northeast monsoon (NEM) and southwest monsoon (SWM), respectively. Shaded boxes indicate the approximate isotopic ranges of fossil-fuel, C_3 biomass, and C_4 biomass endmembers based on previous studies (Budhavant et al., 2023). The isotope signatures indicate temporal variability in the relative contributions of fossil and contemporary carbon sources, providing complementary evidence for changes in aerosol source characteristics over the equatorial Indian Ocean.

https://doi.org/10.5194/egusphere-2026-4276
Preprint. Discussion started: 20 August 2026

The $\Delta^{14}C$ signatures indicate substantial variability in the relative contributions of fossil and contemporary carbon among the analysed samples, while $\delta^{13}C$ provides additional information on carbon source characteristics and atmospheric processing. Together, the isotope measurements demonstrate that carbonaceous aerosols reaching MCOG originate from mixed sources whose relative importance varies over time. However, because only a limited number of samples were analysed, the dataset does not permit a quantitative assessment of seasonal source apportionment or a clear separation of source influences from atmospheric processing based on isotopes alone.

3.5 Broader implications for aerosol–climate interactions over the Indian Ocean

The combined meteorological, transport, chemical, optical, and isotope observations presented in this study provide a coherent picture of how seasonal monsoon circulation regulates carbonaceous aerosols over the equatorial Indian Ocean. The seasonal reversal of the South Asian monsoon controls the origin of air masses reaching MCOG, producing statistically significant changes in aerosol loading and chemical composition while simultaneously altering the relative influence of continental and marine aerosol sources.

The unique location of MCOG between the continental outflow from South and Southeast Asia and the relatively pristine southern Indian Ocean makes it an important receptor site for investigating aerosol evolution during long-range transport (Budhavant et al., 2024). The observations demonstrate a progressive transition from a continentally influenced aerosol regime during the NEM to a more marine-influenced environment during the SWM, with the pre- and post-monsoon periods exhibiting intermediate characteristics as the regional circulation evolves.

Although aerosol loading, chemical composition, and several diagnostic source indicators varied significantly between the two monsoon seasons, BC-MAC_{658} exhibited only modest seasonal variability. This result suggests that monsoon circulation exerts a much stronger influence on aerosol abundance and composition than on the average light-absorbing efficiency of BC particles. While the observed BC-MAC_{658} values are consistent with previous studies of aged aerosols over the Indian Ocean, the present dataset does not provide statistically conclusive evidence that atmospheric aging alone produced enhanced BC absorption during the SWM.

These findings have important implications for regional chemical transport and Earth system models. The observations indicate that accurately representing monsoon-driven transport, wet scavenging, and seasonal changes in aerosol composition is likely to have a greater influence on reproducing the observed variability than introducing increasingly complex parameterizations of BC absorption efficiency. At the same time, the consistency of the measured BC-MAC_{658} values with previous regional observations suggests that continued investigation of transport-dependent changes in BC optical properties remains warranted.

The limited isotope dataset further highlights both the complexity of carbonaceous aerosol sources over the equatorial Indian Ocean and the practical challenges associated with radiocarbon analysis, which requires relatively large carbon masses and substantial analytical effort. Future studies combining long-term chemical measurements, expanded dual-carbon isotope observations, single-particle characterization, and regional modelling will provide stronger constraints on aerosol transport, atmospheric processing, and aerosol–climate interactions across the Indian Ocean.

https://doi.org/10.5194/egusphere-2026-4276
Preprint. Discussion started: 20 August 2026

4. Conclusions

This study presents the first integrated year-round observations of $PM_{2.5}$ chemical composition, aerosol optical properties, air-mass transport, and dual-carbon isotope signatures at the MCOG, providing new insights into the evolution of carbonaceous aerosols over the equatorial Indian Ocean. The combined observations demonstrate that seasonal monsoon circulation is the dominant control on aerosol transport, loading, and chemical composition over this climatically important receptor region.

During the NEM, continental outflow from South and Southeast Asia resulted in significantly higher $PM_{2.5}$, BC, OC, and nss-SO_4^{2-} concentrations, reflecting the long-range transport of combustion-derived aerosols. In contrast, the SWM was characterized by marine air masses, stronger precipitation, and substantially lower aerosol loading, leading to a transition from a continentally influenced aerosol regime to a more marine-dominated environment. Diagnostic aerosol ratios further confirmed systematic seasonal changes in aerosol source characteristics and chemical composition, while the pre- and post-monsoon transition periods exhibited intermediate conditions associated with the seasonal evolution of regional circulation.

Although aerosol loading and chemical composition changed markedly between the two monsoon seasons, BC-MAC_{658} exhibited only modest seasonal variability, with no statistically significant difference between the NEM and SWM. This finding suggests that monsoon circulation exerts a much stronger influence on aerosol abundance and composition than on the average light-absorbing efficiency of BC particles. The observed BC-MAC_{658} values are nevertheless consistent with previous measurements over the Indian Ocean and South Asian outflow, indicating that the optical properties of BC over MCOG are representative of the regional background aerosol.

The limited dual-carbon isotope dataset provided complementary evidence that carbonaceous aerosols reaching MCOG originated from mixed fossil and contemporary sources, although the number of samples was insufficient for quantitative seasonal source apportionment.

Overall, this study demonstrates the value of integrating meteorological observations, transport analysis, aerosol chemistry, optical measurements, and isotope techniques to investigate aerosol evolution over the equatorial Indian Ocean. These multi-constraint observations provide an important observational benchmark for evaluating regional chemical transport and Earth system models. Future long-term observations integrating expanded dual-carbon isotope measurements, direct characterization of BC mixing state, aerosol optical properties, and regional modelling will provide stronger constraints on aerosol transport, atmospheric processing, aerosol–radiation interactions, and their implications for the South Asian monsoon and regional climate.

Data availability.

The datasets generated and analysed during this study will be archived in a public repository upon acceptance of the manuscript. During the review process, the data are available from the corresponding authors upon reasonable request.

https://doi.org/10.5194/egusphere-2026-4276
Preprint. Discussion started: 20 August 2026

Supplement.

Additional information is available in the supplementary materials.

Author contributions.

K.B. and Ö.G. conceived and designed the study. A.M., K.B., and J.R. conducted field sampling and collected aerosol samples at the Maldives Climate Observatory at Gan (MCOG). K.B. performed the chemical analyses, satellite data analysis, and statistical analysis. K.B., J.B., S.K.S., and Ö.G. interpreted the data. K.B. prepared all figures and tables and wrote the first draft of the manuscript. All authors contributed to the interpretation of the results, reviewed and revised the manuscript, and approved the final version for publication.

Acknowledgment

We gratefully acknowledge Mr. Mohamed Nazmee for his invaluable support with field sampling and observatory operations. We also sincerely thank the Maldives Meteorological Service (MMS) and the Government of the Republic of Maldives for their continued support of the joint operation of the Maldives Climate Observatory at Gan (MCOG).

Financial support.

This research has been supported by the Svenska Forskningsrådet Formas (grant no. 2020-01917 to ÖG) and the Vetenskapsrådet (grant nos. 2017-01601 and 2020-05384 to ÖG).

Competing interests. The contact author has declared that none of the authors has any competing interests.

References

Aggarwal, S. G. and Kawamura, K.: Molecular distributions and stable carbon isotopic compositions of dicarboxylic acids and related compounds in aerosols from Sapporo, Japan: implications for photochemical aging during long-range atmospheric transport, *J. Geophys. Res.-Atmos.*, **113**, D14301, https://doi.org/10.1029/2007JD009365, 2008.

Andersson, A., Deng, J., Du, K., Zheng, M., Yan, C., Sköld, M., and Gustafsson, Ö.: Regionally varying combustion sources of the January 2013 severe haze events over eastern China, *Environ. Sci. Technol.*, **49**, 2038–2043, https://doi.org/10.1021/es503855e, 2015.

Bond, T. C., Doherty, S. J., Fahey, D. W., Forster, P. M., Berntsen, T., DeAngelo, B. J., Flanner, M. G., Ghan, S., Kärcher, B., Koch, D., Kinne, S., Kondo, Y., Quinn, P. K., Sarofim, M. C., Schultz, M. G., Schulz, M., Venkataraman, C., Zhang, H., Zhang, S., Bellouin, N., Guttikunda, S. K., Hopke, P. K., Jacobson, M. Z., Kaiser, J. W., Klimont, Z., Lohmann, U., Schwarz, J. P.,

https://doi.org/10.5194/egusphere-2026-4276
Preprint. Discussion started: 20 August 2026

Shindell, D., Storelvmo, T., Warren, S. G., and Zender, C. S.: Bounding the role of black carbon in the climate system: A scientific assessment, *J. Geophys. Res.-Atmos.*, **118**, 5380–5552, https://doi.org/10.1002/jgrd.50171, 2013.

Bosch, C., Andersson, A., Kirillova, E. N., Budhavant, K., Tiwari, S., Praveen, P. S., Russell, L. M., Beres, N. D., Ramanathan, V., and Gustafsson, Ö.: Source-diagnostic dual-isotope composition and optical properties of water-soluble black and elemental carbon in the South Asian outflow intercepted over the Indian Ocean, *J. Geophys. Res.-Atmos.*, **119**, 11743–11759, https://doi.org/10.1002/2014JD022127, 2014.

Budhavant, K., Andersson, A., Bosch, C., Kruså, M., Kirillova, E. N., Sheesley, R. J., Safai, P. D., Rao, P. S. P., and Gustafsson, Ö.: Radiocarbon-based source apportionment of elemental carbon aerosols at two South Asian receptor observatories over a full annual cycle, *Environ. Res. Lett.*, **10**, 064004, https://doi.org/10.1088/1748-9326/10/6/064004, 2015.

Budhavant, K., Andersson, A., Holmstrand, H., Bikkina, P., Bikkina, S., Satheesh, S. K., and Gustafsson, Ö.: Enhanced light absorption of black carbon in rainwater compared with aerosols over the northern Indian Ocean, *J. Geophys. Res.-Atmos.*, **125**, e2019JD031246, https://doi.org/10.1029/2019JD031246, 2020.

Budhavant, K., Andersson, A., Holmstrand, H., Satheesh, S. K., and Gustafsson, Ö.: Black carbon aerosols over the Indian Ocean have unique source fingerprints and optical characteristics during the monsoon season, *Proc. Natl. Acad. Sci. USA*, **120**, e2210005120, https://doi.org/10.1073/pnas.2210005120, 2023.

Budhavant, K., Bikkina, S., Andersson, A., Asmi, E., Kesti, J., Zahid, H., Satheesh, S. K., and Gustafsson, Ö.: Anthropogenic fine aerosols dominate the wintertime regime over the northern Indian Ocean, *Tellus B*, **70**, 1464871, https://doi.org/10.1080/16000889.2018.1464871, 2018.

Budhavant, K., Manoj, M. R., Nair, H. R. C. R., Gaita, S. M., Holmstrand, H., Salam, A., Muslim, A., Satheesh, S. K., and Gustafsson, Ö.: Changing optical properties of black carbon and brown carbon aerosols during long-range transport from the Indo-Gangetic Plain to the equatorial Indian Ocean, *Atmos. Chem. Phys.*, **24**, 11911–11925, https://doi.org/10.5194/acp-24-11911-2024, 2024.

Clarke, S., Holmstrand, H., Budhavant, K., Remani, M., Haslett, S., Rodiouchkina, K., Kooijman, E., and Gustafsson, Ö.: Isotopic apportionment of sulfate aerosols between natural and anthropogenic sources in the outflow of South Asia, *Atmos. Chem. Phys.*, **26**, 5333–5343, https://doi.org/10.5194/acp-26-5333-2026, 2026.

Corrigan, C. E., Ramanathan, V., and Schauer, J. J.: Impact of monsoon transition on the physical and optical properties of aerosols, *J. Geophys. Res.-Atmos.*, **111**, D18208, https://doi.org/10.1029/2005JD006370, 2006.

Das, R., Granat, L., Leck, C., Praveen, P. S., and Rodhe, H.: Chemical composition of rainwater at Maldives Climate Observatory at Hanimaadhoo (MCOH), *Atmos. Chem. Phys.*, **11**, 3743–3755, https://doi.org/10.5194/acp-11-3743-2011, 2011.

Dasari, S., Andersson, A., Bikkina, S., Holmstrand, H., Budhavant, K., Satheesh, S., Backman, J., Kesti, J., Asmi, E., Salam, A., Bisht, D. S., Tiwari, S., Zahid, A., and Gustafsson, Ö.: Photochemical degradation affects the light absorption of water-soluble brown carbon in the South Asian outflow, *Sci. Adv.*, **5**, eaau8066, https://doi.org/10.1126/sciadv.aau8066, 2019.

Dasari, S., Andersson, A., Stohl, A., Evangeliou, N., Bikkina, S., Holmstrand, H., Budhavant, K., Salam, A., and Gustafsson, Ö.: Source quantification of South Asian black carbon aerosols with isotopes and modelling, *Environ. Sci. Technol.*, **54**, 11771–11779, https://doi.org/10.1021/acs.est.0c02193, 2020.

Draxler, R. R. and Hess, G. D.: An overview of the HYSPLIT_4 modelling system for trajectories, dispersion, and deposition, *Aust. Meteorol. Mag.*, **47**, 295–308, 1998.

https://doi.org/10.5194/egusphere-2026-4276
Preprint. Discussion started: 20 August 2026

Fadnavis, S., Roy, C., Sioris, C. E., Kumar, K. N., and Sabin, T. P.: Tropospheric warming over the northern Indian Ocean caused by South Asian anthropogenic aerosols: possible impact on the upper troposphere and lower stratosphere, *Atmos. Chem. Phys.*, **22**, 7179–7191, https://doi.org/10.5194/acp-22-7179-2022, 2022.

Giles, D. M., Sinyuk, A., Sorokin, M., Schafer, J. S., Smirnov, A., Slutsker, I., Eck, T. F., Holben, B. N., Lewis, J. R., Campbell, J. R., Welton, E. J., Ecklund, R., Alexandrov, M. D., O'Neill, N. T., Pietras, C., Issac, M., Chaikovsky, A., Dubovik, O., and Pinker, R. T.: AERONET Version 3 aerosol optical depth and inversion products: Extent, quality, and consistency, *Atmos. Meas. Tech.*, **12**, 169–209, https://doi.org/10.5194/amt-12-169-2019, 2019.

Gustafsson, Ö. and Ramanathan, V.: Convergence on climate warming by black carbon aerosols, *Proc. Natl. Acad. Sci. USA*, **113**, 4243–4245, https://doi.org/10.1073/pnas.1603570113, 2016.

Gustafsson, Ö., Budhavant, K., Chimurkar, N., Clarke, S., Dreyfus, G., Gong, X., Klimont, Z., Klingmüller, K., Kim, S.-W., Lelieveld, J., Myhre, G., Nair, H. R. C. R., Peng, J., Ramanathan, V., Rana, A., Manoj, M. R., Satheesh, S. K., Venkataraman, C., and Zhang, Q.: Atmospheric black carbon in the climate system, *Nat. Rev. Earth Environ.*, https://doi.org/10.1038/s43017-026-00773-3, 2026.

Gustafsson, Ö., Kruså, M., Zencak, Z., Sheesley, R. J., Granat, L., Engström, E., Praveen, P. S., Leck, C., and Rodhe, H.: Brown clouds over South Asia: Biomass or fossil fuel combustion?, *Science*, **323**, 495–498, https://doi.org/10.1126/science.1164857, 2009.

Holben, B. N., Eck, T. F., Slutsker, I., Tanré, D., Buis, J. P., Setzer, A., Vermote, E., Reagan, J. A., Kaufman, Y. J., Nakajima, T., Lavenu, F., Jankowiak, I., and Smirnov, A.: AERONET—A federated instrument network and data archive for aerosol characterization, *Remote Sens. Environ.*, **66**, 1–16, https://doi.org/10.1016/S0034-4257(98)00031-5, 1998.

Höpner, F., Bender, F. A.-M., Ekman, A. M. L., Praveen, P. S., Bosch, C., Ogren, J. A., Andersson, A., Gustafsson, Ö., and Ramanathan, V.: Vertical profiles of optical and microphysical particle properties above the northern Indian Ocean during CARDEX 2012, *Atmos. Chem. Phys.*, **16**, 1045–1064, https://doi.org/10.5194/acp-16-1045-2016, 2016.

Hyvärinen, A.-P., Kolmonen, P., Kerminen, V.-M., Virkkula, A., Leskinen, A., Komppula, M., Hatakka, J., Burkhart, J. F., Stohl, A., Aalto, P. P., Kulmala, M., Lehtinen, K. E. J., Viisanen, Y., and Lihavainen, H.: Aerosol black carbon at five background measurement sites over Finland, a gateway to the Arctic, *Atmos. Environ.*, **45**, 4042–4050, https://doi.org/10.1016/j.atmosenv.2011.04.026, 2011.

IPCC: *Climate Change 2021: The Physical Science Basis. Contribution of Working Group I to the Sixth Assessment Report of the Intergovernmental Panel on Climate Change*, Cambridge University Press, Cambridge, UK and New York, NY, USA, https://doi.org/10.1017/9781009157896, 2021.

Kanamitsu, M.: Description of the NMC Global Data Assimilation and Forecast System, *Weather Forecast.*, **4**, 335–342, https://doi.org/10.1175/1520-0434(1989)004, 1989.

Keene, W. C., Pszenny, A. A. P., Galloway, J. N., and Hawley, M. E.: Sea-salt corrections and interpretation of constituent ratios in marine precipitation, *J. Geophys. Res.-Atmos.*, **91**, 6647–6658, https://doi.org/10.1029/JD091iD06p06647, 1986.

Kesti, J., Heikkinen, P., Asmi, E., Lehtipalo, K., Komppula, M., Portin, H., Lampilahti, J., Backman, J., Hyvärinen, A.-P., Kivekäs, N., Lihavainen, H., and Petäjä, T.: Changes in aerosol size distributions over the Indian Ocean during different meteorological conditions, *Tellus B*, **72**, 1792756, https://doi.org/10.1080/16000889.2020.1792756, 2020.

Kirillova, E. N., Andersson, A., Sheesley, R. J., Kruså, M., Praveen, P. S., Budhavant, K., Safai, P. D., Rao, P. S. P., and Gustafsson, Ö.: ^13C- and ^14C-based study of sources and atmospheric processing of water-soluble organic carbon (WSOC) in South Asian aerosols, *J. Geophys. Res.-Atmos.*, **118**, 614–626, https://doi.org/10.1002/jgrd.50130, 2013.

https://doi.org/10.5194/egusphere-2026-4276
Preprint. Discussion started: 20 August 2026

Kirillova, E. N., Andersson, A., Tiwari, S., Srivastava, A. K., Bisht, D. S., and Gustafsson, Ö.: Water-soluble organic carbon aerosols during a full New Delhi winter: Isotope-based source apportionment and optical properties, *J. Geophys. Res.-Atmos.*, **119**, 3476–3485, https://doi.org/10.1002/2013JD020041, 2014.

Kirillova, E. N., Sheesley, R. J., Andersson, A., and Gustafsson, Ö.: Natural abundance ^13C and ^14C analysis of water-soluble organic carbon (WSOC) in atmospheric aerosols, *Anal. Chem.*, **82**, 7973–7978, https://doi.org/10.1021/ac1014436, 2010.

Kompalli, S. K., Babu, S. S., Moorthy, K. K., Satheesh, S. K., Gogoi, M. M., Nair, V. S., Jayachandran, V. N., Liu, D., Flynn, M. J., and Coe, H.: Mixing state of refractory black carbon aerosol in the South Asian outflow over the northern Indian Ocean during winter, *Atmos. Chem. Phys.*, **21**, 9173–9199, https://doi.org/10.5194/acp-21-9173-2021, 2021.

Lawrence, M. G. and Lelieveld, J.: Atmospheric pollutant outflow from southern Asia: A review, *Atmos. Chem. Phys.*, **10**, 11017–11096, https://doi.org/10.5194/acp-10-11017-2010, 2010.

Li, Z., Lau, W. K.-M., Ramanathan, V., Wu, G., Ding, Y., Manoj, M. G., Liu, J., Qian, Y., Li, J., Zhou, T., Fan, J., Rosenfeld, D., Ming, Y., Wang, Y., Huang, J., Wang, B., Xu, X., Lee, S.-S., Cribb, M., Zhang, F., Yang, X., Zhao, C., Takemura, T., Wang, K., Xia, X., Yin, Y., Zhang, H., Guo, J., Zhai, P. M., Sugimoto, N., Babu, S. S., and Brasseur, G. P.: Aerosol and monsoon climate interactions over Asia, *Rev. Geophys.*, **54**, 866–929, https://doi.org/10.1002/2015RG000500, 2016.

Nair, H. R. C. R., Budhavant, K., Manoj, M. R., Kirillova, E. N., Satheesh, S. K., and Gustafsson, Ö.: Roles of water-soluble aerosol coatings for the enhanced radiative absorption of black carbon over South Asia and the northern Indian Ocean, *Sci. Total Environ.*, **926**, 171721, https://doi.org/10.1016/j.scitotenv.2024.171721, 2024.

Nair, H., Budhavant, K., Manoj, M. R., Andersson, A., Satheesh, S. K., Ramanathan, V., and Gustafsson, Ö.: Aerosol demasking enhances climate warming over South Asia, *npj Clim. Atmos. Sci.*, **6**, 39, https://doi.org/10.1038/s41612-023-00367-6, 2023.

Novakov, T., Andreae, M. O., Gabriel, R., Kirchstetter, T. W., Mayol-Bracero, O. L., and Ramanathan, V.: Origin of carbonaceous aerosols over the tropical Indian Ocean: Biomass burning or fossil fuels?. Geophys. Res. Lett., 27(24), 4061-4064, https://doi.org/10.1029/2000GL011759, 2000.

Nair, V. S., Babu, S. S., and Moorthy, K. K.: Aerosol characteristics in the marine atmospheric boundary layer over the Bay of Bengal and Arabian Sea during ICARB: Spatial distribution and latitudinal/longitudinal gradients, *J. Geophys. Res.-Atmos.*, **113**, D11210, https://doi.org/10.1029/2008JD009823, 2008.

Ramana, M. V. and Ramanathan, V.: Abrupt transition from natural to anthropogenic aerosol radiative forcing: Observation at the ABC Maldives Climate Observatory, *J. Geophys. Res.-Atmos.*, **111**, D20207, https://doi.org/10.1029/2006JD007063, 2006.

Ramanathan, V., Crutzen, P. J., Lelieveld, J., Mitra, A. P., Althausen, D., Anderson, J., Andreae, M. O., Cantrell, W., Cass, G. R., Chung, C. E., Clarke, A. D., Coakley, J. A., Dulac, F., Heintzenberg, J., Heymsfield, A. J., Holben, B., Howell, S., Hudson, J., Jayaraman, A., Kiehl, J. T., Krishnamurti, T. N., Lubin, D., McFarquhar, G., Novakov, T., Ogren, J. A., Podgorny, I., Prather, K., Priestley, K., Prospero, J. M., Quinn, P. K., Rajeev, K., Rasch, P., Rupert, S., Sadourny, R., Satheesh, S. K., Sheridan, P., Valero, F. P. J., and Xu, Y.: Indian Ocean Experiment: An integrated analysis of the climate forcing and effects of the great Indo-Asian haze, *J. Geophys. Res.-Atmos.*, **106**, 28371–28398, https://doi.org/10.1029/2001JD900133, 2001.

Safai, P. D., Budhavant, K. B., Rao, P. S. P., Ali, K., and Sinha, A.: Source characterization for aerosol constituents and changing roles of calcium and ammonium aerosols in the neutralization of aerosol acidity at a semi-urban site in SW India, Atmos. Res., **98**, 78–88, https://doi.org/10.1016/j.atmosres.2010.05.011, 2010

Satheesh, S. K. and Moorthy, K. K.: Radiative effects of natural aerosols: A review, *Atmos. Environ.*, **39**, 2089–2110, https://doi.org/10.1016/j.atmosenv.2004.12.029, 2005.

https://doi.org/10.5194/egusphere-2026-4276
Preprint. Discussion started: 20 August 2026

582 Sheesley, R. J., Kirillova, E. N., Andersson, A., Kruså, M., Praveen, P. S., Budhavant, K., Safai, P. D., Rao, P. S. P., and
583 Gustafsson, Ö.: Year-round radiocarbon-based source apportionment of carbonaceous aerosols at two background sites in South
584 Asia, *J. Geophys. Res.-Atmos.*, **117**, D10202, https://doi.org/10.1029/2011JD017161, 2012.

585 Stein, A. F., Draxler, R. R., Rolph, G. D., Stunder, B. J. B., Cohen, M. D., and Ngan, F.: NOAA's HYSPLIT atmospheric transport
586 and dispersion modeling system, *Bull. Am. Meteorol. Soc.*, **96**, 2059–2077, https://doi.org/10.1175/BAMS-D-14-00110.1, 2015.

587 Stone, E. A., Lough, G. C., Schauer, J. J., Praveen, P. S., Corrigan, C. E., and Ramanathan, V.: Understanding the origin of black
588 carbon in the atmospheric brown cloud over the Indian Ocean, *J. Geophys. Res.-Atmos.*, **112**, D22S23,
589 https://doi.org/10.1029/2006JD008118, 2007.

590 Turpin, B. J. and Lim, H.-J.: Species contributions to $PM_{2.5}$ mass concentrations: Revisiting common assumptions for estimating
591 organic mass, *Aerosol Sci. Technol.*, **35**, 602–610, https://doi.org/10.1080/02786820120648, 2001.

592 Weingartner, E., Saathoff, H., Schnaiter, M., Streit, N., Bitnar, B., and Baltensperger, U.: Absorption of light by soot particles:
593 Determination of the absorption coefficient using Aethalometers, J. Aerosol. Sci., 34, 1445–1463, https://doi.org/10.1016/S0021-
594 8502(03)00359–8 , 2003.